# Storage capacity of two-dimensional neural networks

Shinsuke Koyama*
*Complex Systems Engineering, Graduate School of Engineering, Hokkaido University, N13-W8, Kita-ku, Sapporo 8628, Japan*
(Received 8 May 2001; revised manuscript received 28 September 2001; published 19 December 2001)

We investigate the maximum number of embedded patterns in the two-dimensional Hopfield model. The grand state energies of two specific network states, namely, the energies of the pure-ferromagnetic state and the state of specific one stored pattern are calculated exactly in terms of the correlation function of the ferromagnetic Ising model. We also investigate the energy landscape around them and the stability of the pure retrieval state. Taking into account the qualitative features of the phase diagrams obtained by Nishimori, Whyte, and Sherrington [Phys. Rev. E **51**, 3628 (1995)], we conclude that the network cannot retrieve more than three patterns.

DOI: 10.1103/PhysRevE.65.016124 PACS number(s): 02.50.−r

## I. INTRODUCTION

The Hopfield model [1] is one of the simplest mathematical models which explains associative memory. This model is characterized by binary state neurons and each neuron is represented by Ising spin. In this model system, arbitrary two neurons interact with each other *via* the so-called Hebb rule. The Hebb rule is one of the standard learning rules of the patterns $\xi_i^\mu$ $(i=1,\ldots,N;\ \mu=1,\ldots,p)$ and determines the strength of the interaction $J_{ij}$ between the $i$ and $j$th neurons, say, $S_i$ and $S_j$, as

$$J_{ij}=\frac{1}{N}\sum_\mu \xi_i^\mu \xi_j^\mu, \tag{1}$$

where $\mu$ means the number of embedded patterns and $N$ denotes the number of neurons. These features have been deeply investigated by statistical mechanics [2,3]. Actually, up to now, various extensions and generalizations of the Hopfield model were proposed and these properties were investigated from a statistical mechanical point of view (see, for example [3]). However, little is known about the properties of the Hopfield model in which the length of interactions $J_{ij}$ is restricted to the nearest-neighbor neurons. By the analogy to the spin system in statistical mechanics, we call this type of the Hopfield model the *finite-dimensional Hopfield model*. Inspired by the study of Nishimori *et al.* [4], in this paper, we consider the finite-dimensional Hopfield model storing structured patterns. In general, it is hard to analyze such finite-dimensional systems explicitly. However, one can derive several rigorous results of thermodynamic properties of the system with the assistance of the Pierls arguments and the gauge transformations [4]. Although the qualitative features of the phase diagrams of the system became clear by these analyses, nobody has yet succeeded in deriving their quantitative behavior at all. In this paper, we analyze the storage capacity of the system quantitatively. We restrict ourselves to the case of two-dimensional system on the square lattice.

This paper is organized as follows. In Sec. II, we explain our model system. In Sec. III, we briefly review the qualitative features of the phase diagram obtained by Nishimori *et al.* [4]. In Sec. IV, we analyze the storage capacity of our model system. Section V is devoted to discussion of all the results that we obtain.

## II. DEFINITION OF THE SYSTEM

In this section, we define our model systems. The Hamiltonian of the system is given as

$$H=-\sum_{\langle ij\rangle} J_{ij}S_iS_j, \tag{2}$$

where $S_i$ $(i=1,\ldots,N)$ are the states of the neuron taking binary value $\pm 1$, and $J_{ij}$ is the strength of the interaction between $S_i$ and $S_j$. The summation $\Sigma_{\langle ij\rangle}$ appearing in Eq. (2) runs over nearest-neighbor neurons on a square lattice. We chose the *short-range* Hebb rule as an interaction which is given by

$$J_{ij}=\frac{1}{\sqrt{p}}\sum_{\mu=1}^{p}\xi_i^\mu\xi_j^\mu \tag{3}$$

for the nearest-neighbor sites $\langle ij\rangle$ and $J_{ij}=0$ otherwise. Here, $p$ is the number of embedded patterns and $\xi_i^\mu=\pm 1$ $(\mu=1,\ldots,p;\ i=1,\ldots,N)$. Let us consider the probability distribution of a set of patterns $\{\xi_i^\mu\}(\equiv\{\xi_i^\mu|i=1,\ldots,N;\mu=1,\ldots,p\})$. We suppose that the probability that arbitrary nearest-neighbor sites of the $\mu$th pattern are $\xi_i^\mu$ and $\xi_j^\mu$, respectively, is proportional to

$$\exp\left(\frac{J_0}{\sqrt{p}}\xi_i^\mu\xi_j^\mu\right), \tag{4}$$

where the parameter $J_0$ controls the degree of the correlation between arbitrary nearest-neighbor sites. Let us write $P(\xi_i^\mu=\xi_j^\mu)$ and $P(\xi_i^\mu=-\xi_j^\mu)$ as the probability of $\xi_i^\mu=\xi_j^\mu$ and $\xi_i^\mu=-\xi_j^\mu$, respectively. Then, the ratio of the former to the later is given by

$$\frac{P(\xi_i^\mu=\xi_j^\mu)}{P(\xi_i^\mu=-\xi_j^\mu)}=\exp\left(\frac{2J_0}{\sqrt{p}}\right). \tag{5}$$

*Electronic address: s_koyama@complex.eng.hokudai.ac.jp

 

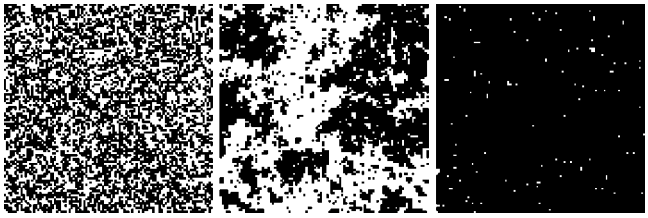

FIG. 1. Typical examples of embedded patterns. The size of patterns is $100\times100$. From the left to the right, the values of parameter $J_0/\sqrt{p}$ are 0.10, 0.42, and 0.60.

For the case of $J_0=0$, Eq. (5) becomes $P(\xi_i^\mu=\xi_j^\mu)=P(\xi_i^\mu=-\xi_j^\mu)$. Hence there is no correlation between $i$ and $j$ sites of $\mu$th patterns and embedded patterns correspond to ''random patterns.'' On the other hand, for the case of $J_0\to\infty$, we obtain $P(\xi_i^\mu=-\xi_j^\mu)=0$. Namely, the value of $\xi_i^\mu$ is same as that of $\xi_j^\mu$ with probability one. Applying Eq. (4) to all nearest-neighbor pairs $\langle ij\rangle$, we obtain the probability distribution for the $\mu$th pattern as

$$\frac{1}{Z_0\left(\frac{J_0}{\sqrt{p}}\right)}\exp\left(\frac{J_0}{\sqrt{p}}\sum_{\langle ij\rangle}\xi_i^\mu\xi_j^\mu\right), \tag{6}$$

where $Z_0(J_0/\sqrt{p})$ is the normalization factor given by

$$Z_0\left(\frac{J_0}{\sqrt{p}}\right)=\sum_{\{\xi_i\}}\exp\left(\frac{J_0}{\sqrt{p}}\sum_{\langle ij\rangle}\xi_i\xi_j\right). \tag{7}$$

Supposing that each pattern is generated by Eq. (6) independently, a set of embedded patterns $\{\xi_i^\mu\}$ is generated by the following probability distribution:

$$P(\{\xi_i^\mu\})=c\prod_{\mu=1}^{p}\exp\left(\frac{J_0}{\sqrt{p}}\sum_{\langle ij\rangle}\xi_i^\mu\xi_j^\mu\right). \tag{8}$$

Here, the normalization factor $c$ is given by $\{Z_0(J_0/\sqrt{p})\}^p$. Note that Eq. (6) corresponds to the Boltzmann weight of the two-dimensional ferromagnetic Ising model on the square lattice whose interaction is given by $1/\sqrt{p}$ at temperature $1/J_0$. Hence embedded patterns are the same as snapshots of equilibrium Monte Carlo simulations for it. This Ising model was explicitly solved in [5] and it is known that there is a critical point at $K=K_c=0.44$, where $K$ denotes the ratio of the temperature to the strength of the interaction. This model has a ferromagnetic solution for $J_0/\sqrt{p}>K_c$ and a paramagnetic solution for $J_0/\sqrt{p}<K_c$. From this fact, in our model system, embedded patterns have a long-range order for $J_0>K_c\sqrt{p}$, on the other hand, there is no long-range correlation for $J_0<K_c\sqrt{p}$. Figure 1 shows typical three examples of embedded patterns.

In the next section, we briefly review the features of the phase diagrams of our model systems obtained by Nishimori *et al.* [4].

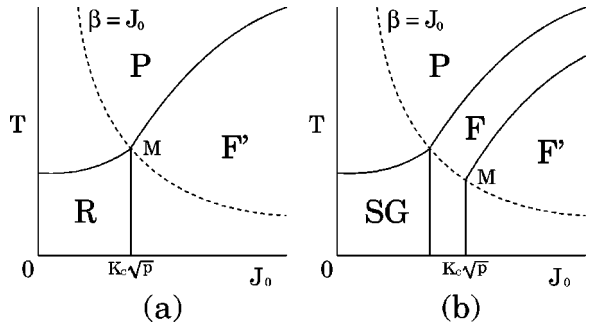


FIG. 2. The qualitative phase diagram with axes of temperature $T$ and a parameter $J_0$ controlling the structure of patterns. The value of $p$ is fixed. (a) For small $p$, there are three phases: paramagnetic $P$, retrieval $R$, and ferromagnetic with finite overlap $F'$. (b) For large $p$, there appears a ferromagnetic phase without retrieval order $F$, and the retrieval phase in the small-$p$ case is replaced by the spin-glass phase.

## III. GENERIC QUALITATIVE PHASE DIAGRAM

Before we explain our analysis of maximum number of embedded patterns, in this section, we briefly review the results by Nishimori *et al.* [4]. Note that their treatments, namely, the gauge transformations and the Peierls arguments are applied to not only the two-dimensional systems but also the systems in arbitrary dimension. Figure 2 shows the qualitative phase diagram with axes of temperature $T$ and a parameter $J_0$ controlling the structure of patterns for a fixed value of $p$. In general, this system has three phases: paramagnetic ($P$), ferromagnetic ($F$), and retrieval ($R$) [or spin glass] phases. Each phase is characterized by the following three-order parameters:

$$q=\frac{1}{N}\sum_{i=1}^{N}\langle S_i\rangle^2, \tag{9}$$

$$m_F=\frac{1}{N}\sum_{i=1}^{N}\langle S_i\rangle, \tag{10}$$

$$m_R=\frac{1}{N}\sum_{i=1}^{N}\xi_i^\mu\langle S_i\rangle, \tag{11}$$

where $\langle\cdots\rangle$ means thermodynamic average. The above three-order parameters $q$, $m_F$, and $m_R$ represent the Edwards-Anderson spin-glass order parameter, the ferromagnetic order parameter, and the overlap between the $\mu$th pattern and the network state $\{S_i\}$, respectively. The paramagnetic, ferromagnetic, retrieval, and spin-glass phase are characterized by the above three-order parameters as $q=m_F=m_R=0$; $q>0, m_F>0$; $q>0, m_R>0$, and $q>0, m_F=m_R=0$, respectively.

Applying the gauge transformations to this system, we obtain the internal energy $[\langle E\rangle]$ and the overlap $[m_R]$ on the lines $\beta(=1/T)=J_0$ in the phase diagram as follows:

$$[\langle E\rangle]=pE_0\left(\frac{\beta}{\sqrt{p}}\right), \tag{12}$$

$$[m_R]=m_0\left(\frac{\beta}{\sqrt{p}}\right), \tag{13}$$

where $E_0(\beta/\sqrt{p})$ is the internal energy of the ferromagnetic Ising model corresponding to the partition function $Z_0(\beta/\sqrt{p})$, and $m_0(\beta/\sqrt{p})$ is the spontaneous magnetization of the same model. Here, the expression of $[\cdots]$ means the average over the distribution (8). Both $E_0(\beta/\sqrt{p})$ and $m_0(\beta/\sqrt{p})$ generally have singularities at some critical point when spatial dimensionality exceeds one. Let us suppose that $\beta/\sqrt{p}=K_c$ is the critical point. Then Eqs. (12) and (13) mean that the internal energy and the overlap of our system have the same singularity at $\beta/\sqrt{p}=K_c$. This implies a phase transition and the boundary between $[m_R]\neq 0$ and $[m_R]=0$ crosses this point on the line $\beta(=1/T)=J_0$ (it is denoted by M in Fig. 2). We should notice that this point is also the critical point of the embedded patterns.

When the value of $p$ is small, a typical phase diagram is given by Fig. 2(a). In this case, it is possible that the retrieval phase exists in the region denoted by $R$. In the same figure, the region $F'$ is the ferromagnetic phase with finite overlap. It is important to notice that this system is not meaningful as an associative memory for $J_0>K_c\sqrt{p}$, since embedded patterns have a long-range ferromagnetic order, as shown on the right-hand side of Fig. 1, and patterns become correlated each other. With this fact in mind, we do not regard this region as a retrieval phase. When the value of $p$ increases, the critical point $J_0=K_c\sqrt{p}$ moves to right. On the other hand, by using the Peierls argument, the ferromagnetic phase still exists in almost the same region. Taking those facts into account, there exists a critical number of patterns $p_c$ above which ($p>p_c$) the ferromagnetic phase is split into two regions, that is, the ferromagnetic phase with finite overlap ($F'$) and the ferromagnetic phase without retrieval order ($F$). At the same time, the retrieval phase in the small-$p$ case is replaced by the spin-glass phase because the region with finite overlap is limited to $F'$ [Fig. 2(b)]. In summary, there exists a critical number of patterns $p_c$ below which ($p<p_c$) the retrieval phase exists there, if any, while for $p>p_c$ the retrieval phase vanishes and this network cannot retrieve embedded patterns.

However, the value of $p_c$ is not yet evaluated quantitatively at all in [4]. Following this section, we investigate it, especially in the case of a two-dimensional system on the square lattice.

## IV. ANALYSIS OF THE SYSTEM

### A. The case of $p=1$

We begin with the case of $p=1$. In this case, the system is identical to the ferromagnetic Ising model and the retrieval solution of the system corresponds to the ferromagnetic solution of the ferromagnetic Ising model. In the case of the square lattice, the critical temperature of the ferromagnetic Ising model is $T_c=2.27$, therefore, the system has a retrieval solution at $T<T_c$.

### B. The case of $p\geqslant 3$

We next analyze the case of $p\geqslant 3$. There is a good evidence to show that the retrieval phase does not exist for this case. Let us start by investigating if there is a state which has a smaller energy than the retrieval state. Substituting $S_i=\xi_i^1$ (for all $i$) into Eq. (2) and averaging it over the distribution (8), we obtain the energy per neuron of the pure retrieval state

$$[E_R]=\frac{1}{N}\left[-\frac{1}{\sqrt{p}}\sum_{\langle ij\rangle}\sum_{\mu=1}^{p}\xi_i^\mu\xi_j^\mu\xi_i^1\xi_j^1\right]$$
$$=-\frac{2}{\sqrt{p}}\left\{1+(p-1)C_1\left(\frac{J_0}{\sqrt{p}}\right)^2\right\}, \tag{14}$$

where $C_1(J_0/\sqrt{p})$ is the nearest-neighbor correlation function of the ferromagnetic Ising model on the square lattice. The explicit form of $C_1$ is

$$C_1\left(\frac{J_0}{\sqrt{p}}\right)=\frac{1}{Z_0\left(\frac{J_0}{\sqrt{p}}\right)}\sum_{\{\xi_i\}}\xi_i\xi_j\exp\left(\frac{J_0}{\sqrt{p}}\sum_{\langle ij\rangle}\xi_i\xi_j\right). \tag{15}$$

We also rewrite the energy per neuron of the pure ferromagnetic state in terms of $C_1(J_0/\sqrt{p})$. Substituting $S_i=1$ (for all $i$) into Eq. (2) and averaging it over the distribution (8), we obtain

$$[E_F]=\frac{1}{N}\left[-\frac{1}{\sqrt{p}}\sum_{\langle ij\rangle}\sum_{\mu=1}^{p}\xi_i^\mu\xi_j^\mu\right]=-2\sqrt{p}C_1\left(\frac{J_0}{\sqrt{p}}\right). \tag{16}$$

We next investigate the properties of the function $C_1(J_0/\sqrt{p})$. It is written in terms of the partition function (7) as follows:

$$C_1\left(\frac{J_0}{\sqrt{p}}\right)=\frac{1}{2N}\frac{\partial\log Z_0(J_0/\sqrt{p})}{\partial(J_0/\sqrt{p})}. \tag{17}$$

It is important to bear in mind that $\log Z_0(J_0/\sqrt{p})$ is explicitly solved in [5] as follows:

$$\frac{1}{N}\log Z_0\left(\frac{J_0}{\sqrt{p}}\right)=\log\left(2\cosh\frac{2J_0}{\sqrt{p}}\right)$$
$$+\frac{1}{2\pi^2}\int_0^\pi\int_0^\pi\log(1-4\kappa\cos\omega_1\omega_2)$$
$$\times d\omega_1\,d\omega_2, \tag{18}$$

where

$$2\kappa=\frac{\tanh(2J_0/\sqrt{p})}{\cosh(2J_0/\sqrt{p})}. \tag{19}$$

Substituting $2\cosh\mu=1/2\kappa|\cos\omega_1|$ into Eq. (18) and using

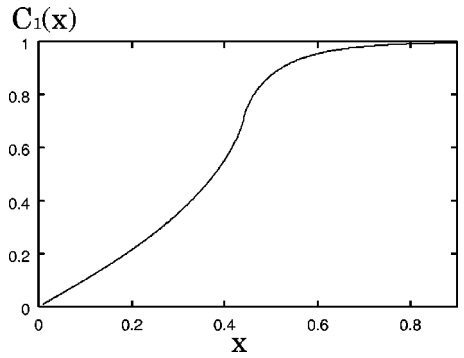


FIG. 3. The shape of the correlation function $C_1(x)$.

$$\int_0^{2\pi} \log(2\cosh\mu - 2\cos\omega)\, d\omega = 2\pi\mu, \tag{20}$$

$$\mu = \cosh^{-1} y = \log(y + \sqrt{y^2-1}), \quad y = \frac{1}{4\kappa|\cos\omega_1|}, \tag{21}$$

we obtain

$$\frac{1}{N}\log Z_0\left(\frac{J_0}{\sqrt{p}}\right) = \log\left(2\cosh\frac{2J_0}{\sqrt{p}}\right) + \frac{1}{2\pi}\int_0^{\pi} \log\frac{1}{2}(1+\sqrt{1-(4\kappa)^2\sin^2\varphi})\, d\varphi. \tag{22}$$

Substituting Eq. (22) into the right-hand side of Eq. (17), explicit solution of $C_1(J_0/\sqrt{p})$ is written by

$$C_1\left(\frac{J_0}{\sqrt{p}}\right) = \frac{1}{2}\coth\frac{2J_0}{\sqrt{p}}\cdot\left(1+\frac{2}{\pi}\kappa_1' L\right), \tag{23}$$

where $L$ is the complete elliptic integral, namely,

$$L = \int_0^{\pi/2} \frac{d\varphi}{\sqrt{1-\kappa_1^2\sin^2\varphi}}, \tag{24}$$

with $\kappa_1 = 4\kappa$ and

$$\kappa_1' = 2\tanh^2\frac{2J_0}{\sqrt{p}} - 1. \tag{25}$$

Figure 3 shows the shape of Eq. (23). From Eqs. (14), (16), and (23), we obtain rigorous values of grand state energies of the pure retrieval and the pure ferromagnetic states.

Now we calculate the condition that the pure ferromagnetic state has a smaller energy than the retrieval state, that is to say, the condition for $[E_R] > [E_F]$. We rewrite this inequality by using Eqs. (14) and (16), then we obtain

$$\frac{1}{p-1} < C_1\left(\frac{J_0}{\sqrt{p}}\right) < 1. \tag{26}$$

As $C_1^{-1}$ is a monotonically increasing function and $C_1^{-1}(1) = \infty$ (see Fig. 3), Eq. (26) leads to

$$\frac{J_0}{\sqrt{p}} > C_1^{-1}\left(\frac{1}{p-1}\right) \equiv U, \tag{27}$$

where $C_1^{-1}$ denotes the inverse of the function $C_1$. We find that the pure ferromagnetic state has a smaller energy than the pure retrieval one as long as this condition is satisfied. As $J_0$ is finite, $p \geqslant 3$ must be satisfied because $C_1^{-1}$ is a monotonically increasing function and $C_1^{-1}(1) = \infty$. Further, it is easy to confirm the following inequality:

$$\frac{\partial([E_F]-[E_R])}{\partial p} < 0. \tag{28}$$

Taking into account $[E_F]-[E_R]<0$ under the condition (27) and $p \geqslant 3$, $[E_F]$ gets smaller relatively as $p$ gets larger. As a result, the pure ferromagnetic state has a smaller energy than the pure retrieval one for $T=0$, $J_0 > U\sqrt{p}$, and $p \geqslant 3$. The value of $U$ is 0.38 for $p=3$, and $U<0.38$ for $p>3$ because of the monotonically increasing property of $C_1^{-1}$. Note that $U$ is always less than $K_c = 0.44$.

We investigate the energy landscape around the pure retrieval state further. Let us calculate the energy increase per interaction when the state changes from the pure retrieval state. The energy stored in an interaction is given by

$$-J_{ij}S_iS_j = -\frac{1}{\sqrt{p}}\sum_{\mu=1}^{p} \xi_i^\mu \xi_j^\mu S_i S_j. \tag{29}$$

Substituting $S_i = \xi_i^1$, $S_j = \xi_j^1$ into Eq. (29), we obtain the energy stored between the $i$th and $j$th neurons of the network retrieving 1th pattern completely. In the same way, substituting $S_i = \xi_i^1$, $S_j = -\xi_j^1$ into Eq. (29) gives the energy of the interaction for the case where the $j$th neuron changes from the retrieval state. Subtracting the former from the latter, and averaging it over the distribution (8), we obtain the energy increase per interaction when the state changes from the retrieval state,

$$[dE_R] = \left[\frac{2}{\sqrt{p}}\sum_{\mu=1}^{p} \xi_i^\mu \xi_j^\mu \xi_i^1 \xi_j^1\right] = \frac{2}{\sqrt{p}}\left\{1+(p-1)C_1\left(\frac{J_0}{\sqrt{p}}\right)^2\right\}. \tag{30}$$

The value of $[dE_R]$ is always positive, and it is expected that the energy increases on the average when the state changes from the pure retrieval state. We estimate the energies of the finite overlap states as follows. Let $n$ be the number of neurons whose states are opposite to the retrieval states. The relation between $n$ and $m_R$ is given by

$$\frac{n}{N} = \frac{1-m_R}{2}. \tag{31}$$

If $n$ is not large, the number of interactions between the retrieval state and opposite state is expected to be about $4n$ because the number of nearest-neighbor neurons is 4 and

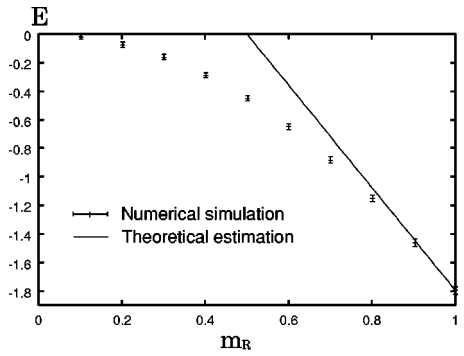


FIG. 4. The average energies $E$ of the retrieval states with overlap $m_R$. The parameter values are $p=3$ and $J_0\sqrt{p}=0.39$. The error bars are results of the numerical simulation in which the size of network is $N=100\times100$, and calculated by averaging of $10^5$ samples. The line shows the result from Eq. (32).

neurons whose states are opposite to the retrieval states lie sparsely in almost all cases. Therefore, the energy of the system per neuron whose overlap is $m_R$ is expected to be

$$[E_{m_R}]=[E_R]+\frac{4n}{N}[dE_R]=[E_R]+2(1-m_R)[dE_R]. \tag{32}$$

Figure 4 shows the result of numerical simulation and compares it with Eq. (32). We set parameter values as $p=3$ and $J_0/\sqrt{p}=0.39$ $(>U)$ at the simulation. We generate $10^5$ sample states for each value of $m_R$ and evaluate $[E_{m_R}]$. Equation (32) agrees with the result of the simulation near $m_R=1$, although it does not agree with the simulations for the case of small $m_R$. This is clearly because the number of interactions between the retrieval state and opposite state is smaller than $4n$ for large $n$. Regardless of it, the energy tends to increase as $m_R$ gets smaller, and the state near $m_R=1$ is likely the smallest energy among the finite overlap states. Almost the same argument can be applied to the ferromagnetic state, and the state near $m_F=1$ is the smallest energy among the ferromagnetic order. Taking into account $[E_R]>[E_F]$, the energy of ferromagnetic order is expected to be smaller than that of retrieval order as long as $p\geqslant3$ and $J_0>U\sqrt{p}$ are satisfied.

We also investigate the stability of the pure retrieval state. The variance of $dE_R$ is given by

$$\begin{aligned}[\{\Delta(dE_R)\}^2]&=[dE_R^2]-[dE_R]^2\\&=\frac{4(p-1)}{p}\left\{1+(p-2)C_1\left(\frac{J_0}{\sqrt{p}}\right)^2\right.\\&\quad\left.-(p-1)C_1\left(\frac{J_0}{\sqrt{p}}\right)^4\right\}.\end{aligned} \tag{33}$$

Using Eqs. (14) and (33), the ratio of $[dE_R]^2$ to this variance is obtained by

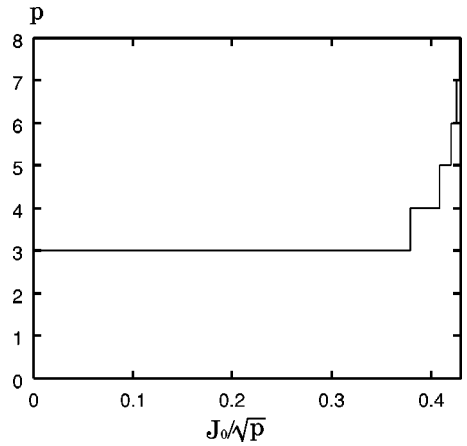


FIG. 5. The minimum value of $p$ that is satisfied with Eq. (36) as a function of the parameter $J_0/\sqrt{p}$, which determines the structure of patterns.

$$\begin{aligned}&\frac{[\{\Delta(dE_R)\}^2]}{[dE_R]^2}\\&=\frac{(p-1)\left\{1+(p-2)C_1\left(\frac{J_0}{\sqrt{p}}\right)^2-(p-1)C_1\left(\frac{J_0}{\sqrt{p}}\right)^4\right\}}{1+2(p-1)C_1\left(\frac{J_0}{\sqrt{p}}\right)^2+(p-1)^2C_1\left(\frac{J_0}{\sqrt{p}}\right)^4}.\end{aligned} \tag{34}$$

Partially differentiating the above equation by $p$ (the value of $C_1$ is fixed), we obtain the following inequality:

$$\frac{\partial}{\partial p}\left(\frac{[\{\Delta(dE_R)\}^2]}{[dE_R]^2}\right)>0. \tag{35}$$

This means that the more the value of $p$ gets large, the more the energy is likely to decrease when the state changes from the retrieval state, although it increases on the average. Therefore, the pure retrieval state becomes unstable for large $p$. We can roughly estimate the value of $p$ for which the pure retrieval state gets unstable by

$$\frac{[\{\Delta(dE_R)\}^2]}{[dE_R]^2}>1. \tag{36}$$

In Fig. 5, we plot the minimum value of $p$ that is satisfied with Eq. (36). For example, Eq. (36) is satisfied with $p\geqslant8$ for $J_0/\sqrt{p}=0.43$. Note that this is probably overestimating and the value of $p$ is likely smaller. We confirm this argument in numerical simulations of the dynamics at $T=0$. Figure 6 shows a typical example of how the overlap $m_R$ depends on the Monte Carlo step in computer simulations, in which $N=100\times100$ and $J_0/\sqrt{p}=0.43$. The state of network starts with the embedded pattern itself. In these simulations, the pure retrieval state is already unstable for $p=3$, and the net-

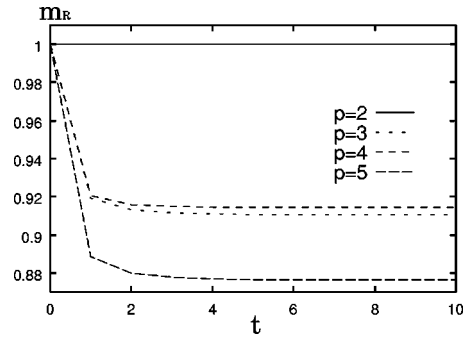


FIG. 6. The typical example of how the overlap $m_R$ depends on the Monte Carlo step $t$ in Monte Carlo simulations at $T=0$. We set the system size and the parameter as $N=100\times100$ and $J_0/\sqrt{p}=0.43$, respectively.

work falls into a certain local minimum near $m_R=1$. This implies that the pure retrieval state is no longer stable for $p\geqslant3$.

Taking all the above results into account, we show that there is no retrieval phase if $p\geqslant3$. As we have seen, $U$ is always smaller than $K_c=0.44$ for $p\geqslant3$, and the ferromagnetic state has smaller energy than the retrieval state for $J_0>U\sqrt{p}$. Moreover, the pure retrieval state is no longer stable for $p\geqslant3$. From those results, we conclude that the region of $J_0>U\sqrt{p}$ at $T=0$ is not a retrieval phase. Therefore, the boundary of $[m_R]=0$ is prohibited from landing at $J_0<K_c\sqrt{p}$ on the $J_0$ axis like $L_2$ in Fig. 7, and it should land at $J_0=K_c\sqrt{p}$ from point $M$ vertically like $L_1$. Hence, there is no retrieval phase in the region $J_0<K_c\sqrt{p}$ (for all $T$) because the region with finite overlap is limited at $J_0>K_c\sqrt{p}$. As a result, the phase diagram should be like Fig. 2(b) and the retrieval phase does not exist for the case of $p\geqslant3$.

### C. The case of $p=2$

For the case of $p=2$, Figs. 5 and 6 imply that the pure retrieval state is stable, although it is possible that there exists a state, except the ferromagnetic state, whose energy is smaller than that of the retrieval state. Hence, the retrieval state is expected to be a stable or metastable one for this case. However, it is very difficult to conclude whether the retrieval state has the minimum energy or not, because the Hamiltonian of this system has a very complicated energy landscape. In order to evaluate the grand state energy of it, we should carry out simulated annealing , for example. However, up to now, we do not yet have reliable results. This will be our future problem.

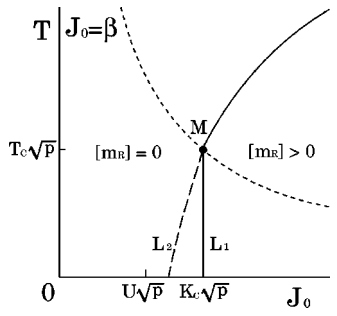


FIG. 7. In the case of $p\geqslant3$, $U$ is smaller than $K_c\sqrt{p}$ and the region of $J_0>U\sqrt{p}$ at $T=0$ is not retrieval phase. Therefore, the boundary of $[m_R]=0$ like $L_2$ is prohibited and it should be like $L_1$.

## V. CONCLUSION

In this paper, we investigated the maximum number of embedded patterns in the two-dimensional Hopfield model storing structured patterns. As a result, we found that there exists the retrieval phase for $p\leqslant2$, however, it does not exist for $p\geqslant3$. In other words, this system cannot retrieve more than three patterns. This result agrees with a consideration of networks with randomly diluted synapses, in which $p_c$ is proportional to the average connectivity per neuron [6]. Namely, we can see from this argument that the value of $p_c$ for our network is finite because the average connectivity per neuron is four (finite number). However, our result is more strict than that from this argument.

Moreover, $p_c=2$ is satisfied with any value of $J_0$, even the conventional ''random patterns.'' In addition, it is known that the storage capacity of the network with spatially correlated patterns is lower than that with random patterns. This implies that the smallness of the value of $p_c$ is due to the dimensionality two of the network rather than the structure of embedded patterns. This argument also implies that although there are several modifications in order to improve storage capacity with spatially correlated patterns (see [7], for example), these modifications are not expected to be remarkable improvements for our model system.

From all the above arguments, we conclude that storage capacity of associative memory is strongly restricted by the spatial structure of the network.

## ACKNOWLEDGMENTS

I would like to thank J. Inoue and M. Wada for helpful discussions and encouragements. I also thank H. Nishimori for valuable comments.

[1] J. J. Hopfield, Proc. Natl. Acad. Sci. U.S.A. **79**, 2554 (1982).
[2] D. Amit, H. Gutfreund, and H. Sompolinsky, Phys. Rev. A **32**, 1007 (1985); Phys. Rev. Lett. **55**, 1530 (1985).
[3] J. Hertz, A. Krogh, and R. G. Palmer, *Introduction to the Theory of Neural Computation* (Addison-Wesley, New York, 1991).
[4] H. Nishimori, W. Whyte, and D. Sherrington, Phys. Rev. E **51**, 3628 (1995).
[5] L. Onsager, Phys. Rev. **65**, 117 (1944).
[6] B. Derrida, E. Gardner, and A. Zippelius, Europhys. Lett. **4**, 167 (1987).
[7] M. Schlüter and F. Wagner, Phys. Rev. E **49**, 1690 (1994).